NASA Technical Memorandum 81819

NASA-TM-81819 19800014843

TWINTAN: A PROGRAM FOR TRANSONIC WALL INTERFERENCE ASSESSMENT IN TWO-DIMENSIONAL WIND TUNNELS

William B. Kemp, Jr.

National Aeronautics and Space Administration

Langley Research Center
Hampton, Virginia 23665

SUMMARY

A method for assessing the wall interference in transonic two-dimensional wind tunnel tests has been developed and implemented in a computer program. The method involves three successive solutions of the transonic small disturbance potential equation to define the wind tunnel flow, the perturbation attributable to the model, and the equivalent free air flow around the model. Required input includes pressure distributions on the model and along the top and bottom tunnel walls which are used as boundary conditions for the wind tunnel flow. The wall-induced perturbation field is determined as the difference between the perturbation in the tunnel flow solution and the perturbation attributable to the model. The methodology used in the program is described and detailed descriptions of the computer program input and output are presented. Input and output for a sample case are given in an appendix.

INTRODUCTION

A method has been developed for assessing the wall-induced velocity perturbation existing during transonic airfoil tests in two-dimensional wind tunnels. The method can be considered as a transonic nonlinear counterpart of the classical wall interference theory. The basic principles are outlined in reference 1 and a qualitative description of the method is given in reference 2 along with a discussion and illustration of its capabilities. The present implementation of the method includes some capabilities which were added subsequent to the date of reference 2.

The present paper is intended to serve as a user's guide to the computer program TWINTAN* in which the method has been implemented. This paper presents the methodology used in the program and a detailed description of the input required and the output provided by the program in its present form. Input and output for a sample case are given in an appendix.

The computer program described herein is in an elementary form suitable for evaluation and exploratory use. Current experience with the program leads to the belief that the Mach number correction is generally reliable and that the nonuniformities in the wall-induced perturbation field and their effect on the airfoil pressure distribution are adequately revealed. The accuracy of the angle of attack correction, however, depends directly on the accuracy with which a flow direction reference for the wind tunnel flow computation can be established. It is anticipated that improvements in both accuracy and convenience could result from mutual optimization of this program with the instrumentation and data system of the particular test facility with which it is to be used.

---

*Program TWINTAN is distributed through COSMIC, Computer Software Management and Information Center, 112 Barrow Hall, University of Georgia, Athens, GA 30602.

SYMBOLS

a	coefficient of ϕ_y in boundary condition expressions
A,B,C,D	coefficients in tridiagonal form of governing equation
B',D'	coefficients in line relaxation algorithm
c	airfoil chord
c_l	section lift coefficient
f	transformation derivative in longitudinal direction
g	transformation derivative in transverse direction
j	longitudinal grid index, also longitudinal computational coordinate
k	transverse grid index, also transverse computational coordinate
M	Mach number
n	stretching parameter in coordinate transformation
P,Q	quantities in the finite difference formulation of the governing equation
q	dynamic pressure
s	distance along airfoil surface
U	longitudinal velocity of uniform flow
V	resultant velocity
x	longitudinal physical coordinate
y	transverse physical coordinate
z	general physical coordinate
α	angle of attack
Γ	circulation
γ	ratio of specific heats
Δ	prefix denoting an increment
δ	scaling parameter in coordinate transformation

ζ general computational coordinate

Λ coefficient of longitudinal term in governing equation

μ switching parameter in finite difference formulation of the governing equation

Φ total velocity potential

ϕ dimensionless perturbation velocity potential

Subscripts:

x,y denote partial differentiation with respect to x or y

j,k denote value at j-th or k-th grid line

R wind tunnel reference conditions

∞ corrected far field conditions

METHODOLOGY

The procedure implemented in program TWINTAN involves three successive finite-difference solutions to the two-dimensional transonic small disturbance potential equation. The first solution is a calculation of the flow around the test airfoil in the wind tunnel. Pressure distributions measured during the test to be assessed, both on the airfoil and at the upper and lower walls, are imposed as boundary conditions to enhance the fidelity of reproduction of the actual tunnel flow. The assumptions and inaccuracies usually encountered in modeling the ventilated walls and the remaining tunnel geometry are thereby avoided.

The second solution is a calculation of the flow perturbation attributable to the model. Free air outer boundary conditions are used and the model boundary conditions are imposed in the form of singularity distributions extracted from the tunnel flow solution. The wall-induced perturbation is then determined as the difference between the perturbations calculated in the two flow solutions. In order to keep the nonlinear effects comparable, the streamwise component of the wall-induced perturbation at a user specified match point is evaluated iteratively during the second solution and is transferred as a correction to the far field velocity. Upon convergence of the second solution, the wall-induced corrections to Mach number and free-stream static and dynamic pressures are thereby fixed.

The third solution is a calculation of the free-air flow at the corrected free-stream Mach number around the equivalent airfoil shape determined in the tunnel flow solution. The test lift coefficient, corrected by the dynamic pressure ratio, is specified and the angle of attack adjusted to satisfy the

Kutta condition. The results include a specific value for the angle-of-attack correction and a pressure distribution which could be considered fully corrected for wall interference if it does not depart excessively from the original airfoil pressure distribution reduced according to the corrected free-stream conditions. Some features of the method are described in detail in the following sections to aid the user in adapting the program to a specific facility as well as in making refinements.

Governing Equation

The dependent variable in each of the flow solutions of the present program is the dimensionless perturbation potential ϕ which is related to a total dimensional velocity potential Φ by

$$\Phi = U_R\, c\left(\frac{U_\infty}{U_R}\frac{x}{c} + \phi\right) \tag{1}$$

where U_R is the velocity corresponding to the tunnel reference Mach number. For the tunnel flow solution U_∞ is set equal to U_R but during the model perturbation solution U_∞ is updated by adding the wall induced blockage velocity. The updated value is used for the equivalent free air solution. Thus, by equation (1) ϕ is scaled to the same units in all solutions while representing the perturbation from uniform flows of different velocities.

The perturbation potential is governed by an extended form of the transonic small disturbance equation expressed as

$$\Lambda\frac{\partial^2\phi}{\partial x^2} + \frac{\partial^2\phi}{\partial y^2} = 0 \tag{2}$$

where

$$\Lambda = 1 - M_\infty{}^2 - (\gamma + 1)\, M_\infty{}^2\frac{U_R}{U_\infty}\frac{\partial\phi}{\partial x}\left(1 + \frac{U_R}{2U_\infty}\frac{\partial\phi}{\partial x}\right)$$

The higher order term in Λ is included to improve the accuracy of velocity equivalence between the perturbation and the far field and thereby suppress spurious errors which were otherwise observed when U_R/U_∞ differed significantly from unity.

The conservative form finite difference approximation to equation (2) used in the program is described by the following expressions:

$$\frac{\partial^2\phi}{\partial y^2} = g_k\left[\left(\frac{\partial\phi}{\partial y}\right)_{j,k+\frac{1}{2}} - \left(\frac{\partial\phi}{\partial y}\right)_{j,k-\frac{1}{2}}\right]$$

$$\Lambda \frac{\partial^2 \phi}{\partial x^2} = f_j \left[\left(1 - \mu_j \right) P_j + \mu_{j-1} P_{j-1} \right]$$

$$P_j = \Lambda_j \left[\left(\frac{\partial \phi}{\partial x} \right)_{j+\frac{1}{2},k} - \left(\frac{\partial \phi}{\partial x} \right)_{j-\frac{1}{2},k} \right]$$

$$\Lambda_j = 1 - M_\infty{}^2 - (\gamma + 1) M_\infty{}^2 \frac{U_R}{U_\infty} Q_j \left(1 + \frac{U_R}{2U_\infty} Q_j \right)$$

$$Q_j = \frac{1}{2} \left[\left(\frac{\partial \phi}{\partial x} \right)_{j+\frac{1}{2},k} + \left(\frac{\partial \phi}{\partial x} \right)_{j-\frac{1}{2},k} \right]$$

$$\mu_j = \begin{cases} 0 \text{ if } \Lambda_j \geq 0 \\ 1 \text{ if } \Lambda_j < 0 \end{cases}$$

$$f_j = \left(\frac{dj}{dx} \right)_j$$

$$g_k = \left(\frac{d|k|}{dy} \right)_k$$

In defining the transformation derivatives f and g, the quantities j and k each serve the dual role of computational variable and grid index because the transformation is scaled so that the mesh size is one unit of the computational variable. The first derivatives of ϕ appearing in the preceding expressions are all formed by single mesh differencing; for example:

$$\left(\frac{\partial \phi}{\partial y} \right)_{j,k+\frac{1}{2}} = g_{k+\frac{1}{2}} \left(\phi_{j,k+1} - \phi_{j,k} \right)$$

Note that at shock points, $\mu_j = 0$ and $\mu_{j-1} = 1$ so the longitudinal term of the governing equation contains the sum of central difference and upwind difference contributions. If the nonconservative form is selected (ICNSV = 0) the upwind difference contribution is omitted at shock points.

In the following discussion, points in the lower half plane will be identified by a negative sign on the k index. Accordingly, $g_{-k} = -g_k$.

The governing equation is arranged in the tridiagonal form

$$A_k \phi_{j,k-1} + B_k \phi_{j,k} + C_k \phi_{j,k+1} = D_k \tag{3}$$

along j = constant lines and is solved by the method of successive line over-relaxation subject to boundary conditions imposed in Dirichlet form at the outer boundary and in various forms at the airfoil. The development of these boundary conditions for the three flow computations is described in subsequent sections. The implicit algorithm used to solve equation (3) along each line is based on the recursive relationship

$$\phi_{j,k} = D'_k + B'_k \phi_{j,k-1} \tag{4}$$

where the coefficients B' and D' are defined by

$$D'_k = \frac{D_k - C_k D'_{k+1}}{B_k + C_k B'_{k+1}}$$

$$B'_k = \frac{-A_k}{B_k + C_k B'_{k+1}}$$

and are calculated recursively starting with the outer boundary condition and proceeding inward to $k = \pm 2$.

Because of the symmetric grid indexing used, the $k = 1$ grid line is treated numerically as a boundary along its entire length. At points ahead of the airfoil and in the wake, the boundary condition is derived from the governing equation. In the wake, the potential jump relation

$$\phi_{j,-1} = \phi_{j,1} - \Gamma \tag{5}$$

is used along with equation (4) applied at $k = \pm 2$ to write equation (3) at $k = 1$ and obtain the solution.

$$\phi_{j,1} = \frac{D_1 - C_1\left[D'_2 + D'_{-2} + \Gamma\left(1 - B'_{-2}\right)\right]}{B_1 + C_1\left(B'_2 + B'_{-2}\right)} \tag{6}$$

Equations (5) and (4) are then used to complete the line solution. The same procedure, but with $\Gamma = 0$, is used ahead of the airfoil.

Boundary Conditions for Tunnel Flow Computation

All input pressure coefficients are interpolated onto the appropriate longitudinal mesh center points, converted to the form of velocity magnitude squared using the exact pressure coefficient definition, and stored in this form. The boundary conditions for the tunnel flow computation are derived primarily from these data.

On the longitudinal outer boundaries at $k = \pm KW$, values of ϕ_x are found from

$$V^2 = \left(1 + \phi_x\right)^2 + \phi_y{}^2 \tag{7}$$

and integrated to determine the boundary values of ϕ. Values of ϕ_y are assumed initially to be zero and then are updated iteratively. The ϕ_x gradients approaching the ends of the upper and lower boundaries are used with the governing equation (2) to find ϕ_{yy} at each boundary corner. At the two upstream corners, ϕ_y is specified by input quantities. The variation of ϕ on the upstream boundary is described as a fourth degree polynomial in y whose coefficients are determined from the values of ϕ_y and ϕ_{yy} noted above and the assumption that $\phi = 0$ at the lower upstream corner. On the downstream boundary, ϕ is defined as a cubic in y with the term $\Gamma/2 \, \mathrm{sgn} y$ added to provide the needed potential jump across the wake. The four coefficients are determined to satisfy the known values of ϕ and ϕ_{yy} at the corners.

The airfoil boundary conditions are imposed in Dirichlet form on a slit at $y = 0$ rather than on the airfoil surface. It is not appropriate to require that the airfoil surface velocities be reproduced on the slit. Instead, we require that the longitudinal distribution of velocity potential on the airfoil surface be reproduced on the slit. Thus,

$$\int V \frac{ds}{dx} \, dx = \int \left(1 + \phi_x\right) dx \tag{8}$$

where V is the airfoil surface velocity determined from the pressure coefficients and ds is the element of surface arc length. The present program calculates ϕ_x by equating the integrands of equation (8) using the approximation

$$\frac{ds}{dx} = \sqrt{1 + \phi_y{}^2}$$

in which ϕ_y is calculated at the slit and is updated iteratively. This procedure may be recognized as an adaptation of the Riegels rule.

The approximations inherent in the above procedure are unacceptable at a blunt leading edge, therefore equation (8) is used to determine ϕ_x for only

those mesh intervals downstream of the leading edge. In the mesh interval bracketing the leading edge, upper and lower surface values of ϕ_x are determined such that two broad constraints are satisfied. The first requires that the total circulation determined by integrating $\Delta\phi_x$ over the entire airfoil chord must correspond to the prescribed lift coefficient. The circulation error is corrected directly by adjusting the $\Delta\phi_x$ in the leading edge interval. The second constraint is the airfoil thickness closure condition which requires that the net source strength determined by integrating $\Delta\phi_y$ over the entire airfoil chord must correspond to the prescribed drag coefficient. This constraint is implemented by allowing the error in net source strength to control the average value of ϕ_x in the leading edge interval. The direct effect of negative ϕ_x at the leading edge is to depress the value of ϕ at the first grid point behind the leading edge, thereby creating source strength at this point. As a secondary effect, however, added source strength is created over the entire chord with a distribution such that the ϕ_x boundary conditions are still satisfied in each mesh interval. The existence of such a source distribution which has no effect on ϕ_x anywhere on the chord line causes the thickness design problem to be ill posed without a specific constraint on thickness closure. The role of the thickness closure constraint in the airfoil thickness design problem is analogous to the role of the Kutta condition in the airfoil lift analysis problem.

Boundary Conditions for Model Perturbation Computation

The purpose of the model perturbation computation is to define that part of the tunnel flow perturbation which is attributable directly to the airfoil. Accordingly, the airfoil boundary condition in this computation should assure that the vorticity and source distributions on the slit representing the airfoil duplicate those existing in the tunnel flow solution. Thus, the quantities

$$\Delta\phi_j = \phi_{j,1} - \phi_{j,-1} \tag{9a}$$

$$\Delta\phi_{yj} = \phi_{yj,1} - \phi_{yj,-1} \tag{9b}$$

as extracted from the tunnel flow solution are to be reproduced in the free air computation.

The values of ϕ_y used in (9b) are those at grid points on the slit. They may be expressed in terms of the ϕ values at surrounding grid points by using a ϕ_{yy} at the slit expressed by the governing equation (2). The results can be written in the following form:

$$B_1\,\phi_{j,1} + C\,\phi_{j,2} = D_1 - a\,\phi_{yj,1} \tag{10a}$$

$$B_{-1}\,\phi_{j,-1} + C\,\phi_{y,-2} = D_{-1} + a\,\phi_{yj,-1} \tag{10b}$$

From equations (10), (9) and (4) we find

$$\phi_{j,1} = \frac{D_1 + D_{-1} - C\left(D'_2 + D'_{-2}\right) + \left(B_{-1} + C\,B'_{-2}\right)\Delta\phi_j - a\Delta\phi_{yj}}{B_1 + B_{-1} + C\left(B'_2 + B'_{-2}\right)} \tag{11}$$

which is used along with equation (9a) to impose the airfoil boundary conditions in the model perturbation computation.

The values of the perturbation potential imposed on the outer boundary of this computation are calculated from a far field analytic expression which includes the two-dimensional lift and thickness integral terms given in reference 3 and an additional term representing the far field influence of the net source strength at the airfoil.

During this computation, the far field Mach number is updated by transferring the wall-induced longitudinal velocity perturbation evaluated at the specified match point into the far field velocity using the following procedure:

$$\frac{U_\infty}{U_R} = 1 + \left(\phi_x\right)_T - \left(\phi_x\right)_M \tag{12}$$

where $\left(\phi_x\right)_T$ is the value of ϕ_x at the match point in the converged tunnel flow solution and $\left(\phi_x\right)_M$ is that in the current iteration step of the model perturbation solution. The updated Mach number is then found from

$$M_\infty{}^2 = \frac{\left(\frac{U_\infty}{U_R}\right)^2 M_R{}^2}{1 + \frac{\gamma - 1}{2} M_R{}^2 \left[1 - \left(\frac{U_\infty}{U_R}\right)^2\right]} \tag{13}$$

The linearized compressibility factor used in calculating the outer boundary conditions is updated along with M_∞.

Boundary Conditions for Equivalent Free Air Computation

The equivalent free air computation is to define the free air flow at the corrected far field Mach number around the equivalent airfoil shape described by the tunnel flow solution at an angle of attack corresponding to the lift measured in the experiment. The lift coefficient based on the free stream conditions at M_∞ is

$$c_{l_\infty} = c_{l_R} \frac{q_R}{q_\infty}$$

where c_{l_R} is based on tunnel reference conditions and

$$\frac{q_\infty}{q_R} = \left(\frac{M_\infty}{M_R}\right)^2 \left(\frac{1 + \frac{\gamma - 1}{2} M_R^2}{1 + \frac{\gamma - 1}{2} M_\infty^2}\right)^{\frac{\gamma}{\gamma-1}}$$

The far field boundary conditions and the potential jump in the wake are determined using

$$\Gamma_\infty = \Gamma_R \frac{U_\infty}{U_R} \frac{q_R}{q_\infty}$$

where the velocity ratio accounts for the fact that Γ (like ϕ) is expressed in units of U_R c.

The airfoil boundary condition is a Neumann condition using values of ϕ_y extracted directly from the tunnel flow solution by use of equation (10). The boundary condition is then formed by combining equation (10) and (4) and allowing for an angle of attack correction $\Delta\alpha$.

$$\phi_{j,\pm 1} = \frac{D_{\pm 1} - C\, D'_{\pm 2} \mp a\left(\phi_{yj,\pm 1} - \Delta\alpha\right)}{B_{\pm 1} + C\, B'_{\pm 2}}$$

where the upper and lower signs refer to the airfoil upper and lower surfaces, respectively.

DESCRIPTION OF INPUT

Program TWINTAN is written in FORTRAN 4 and has been implemented on the CDC CYBER 175 computer with a central memory requirement of approximately 60,000 (octal) of 60 bit words. The program input is provided in two namelist blocks. The first, labeled NPUT, contains 12 parameters to define the computational grid, 6 parameters for problem constraint and 8 parameters for numerical process control. The second block, RDPX, provides arrays of wall and model pressure coefficients and their longitudinal locations. All input data are nondimensional with the airfoil chord assumed to be the unit of length.

Computational Grid Inputs

The perturbation potential is stored by the program in an array addressed as PHI(J, K, L). The index L takes on values of 1 or 2 for the upper or lower half plane respectively. J and K are the longitudinal and lateral indices respectively in each half plane. The physical configuration of the upper half grid is sketched in figure 1. The K = 1 grid line is the axis of grid symmetry between the two half planes and represents the tunnel center line, y = 0. The lower half grid is a mirror image of the upper. The longitudinal grid spacing is uniform from J1 to J4. The longitudinal spacing upstream from J1 and downstream from J4 and the lateral spacing of the entire grid are stretched by transformations of the form.

$$z = n\delta \frac{\zeta}{n - \zeta} \tag{14}$$

where z represents a physical coordinate and ζ is the computational coordinate in the corresponding direction. In the present program, the transformation is truncated to prevent z reaching infinity. Equation (14) is used to relate the coordinate x or y directly to the grid index J or K by assuming a computational mesh interval $\Delta\zeta$ of unity. The stretching parameter n then represents the number of mesh intervals which would cover the range $0 \leq z \leq \infty$, and the scaling parameter δ is the limit as z approaches zero of the physical mesh interval Δz. The specific relations for the upstream and downstream, and lateral transformations are formed by substituting the parameters tabulated below into equation (14).

Index Range	$1 \leq J \leq J1$	$J4 \leq J \leq J5$	$1 \leq K \leq KB$
ζ	J1 - J	J - J4	K - 1
z	x(J1) - x	x - x(J4)	y
n	M	M	N
δ	DXMN	DXMN	DYMN

The program sets the uniform mesh interval Δx in the range from J1 to J4 equal to DXMN, locates J3 at the airfoil trailing edge (x = 1.), and determines J2 such that the airfoil leading edge (x = 0.) lies in the mesh space between J2 and J2 + 1. The boundaries of the uniform longitudinal mesh region are

```
x(J1) = 1. - DXMN * (J3 - J1)

x(J4) = 1. + DXMN * (J4 - J3)
```

The foregoing information is sufficient to determine the physical coordinates x,y of each grid intersection J,K in terms of the following program input parameters. The longitudinal grid used in the free-air computation is defined by the integers J1, J3, J4, J5 and M and the real constant DXMN which must satisfy the following constraints.

$$J5 \leq 100$$

$$J1 \leq M$$

$$J5 - J4 < M$$

$$(J3 - J1) * DXMN \geq 1.$$

$$J4 > J3$$

The grid lines serving as the upstream and downstream boundaries of the tunnel flow computation are denoted by the integers JU and JD respectively which must satisfy:

$$JU \geq 1$$

$$JD \leq J5$$

In addition, all wall boundary points, located at mesh centers from x(JU + 1/2) to x(JD - 1/2) must lie within the longitudinal range of the input wall pressures.

The lateral grid is defined by the integers KB, N and KW and the real constant DYMN which must satisfy:

$$KB \leq 50$$

$$KB \leq N$$

$$KW \leq KB$$

KW identifies the lateral boundary of the tunnel flow computation and must be selected along with N and DYMN such that $\pm$y(KW) is the lateral distance from the tunnel center line to the upper or lower line of input wall pressures.

The following points should be considered also in selecting grid input parameters. The outer boundaries of the free-air computation, x(1), x(J5) and y(KB) should lie several chord lengths from the model for best accuracy of the free-air boundary conditions. If, however, J1 and (J5-J4) closely approach M, and KB closely approaches N, the solution convergence rate is adversely affected.

Problem Constraint Inputs

Five real and one integer input parameters provide constraints needed in the tunnel flow computation. AMREF is the reference Mach number corresponding to the tunnel reference conditions used in reducing the input data to coefficient form. The lift coefficient CL defines the total airfoil circulation. The accuracy of the calculated wall-induced upwash depends on the accuracy of the CL input. CD is the airfoil drag coefficient which provdes the airfoil thickness closure constraint. The integer JP defines the location ($x = x(JP - 1/2)$, $y = 0$) at which the local Mach number in the model perturbation computation is matched to that in the tunnel flow. For low Mach number cases, the results are essentially independent of the choice of JP. For supercritical flows, the match point should be located just upstream of the sonic point in the shock, thereby matching shock strength in the two flows. Numerical divergence might be encountered if the match point is just downstream of a strong shock.

The real parameters SLA and SLB are the onset flow streamline slopes at the upper and lower corners respectively of the upstream boundary of the tunnel flow computation $x(JU)$. The present formulation presumes that this upstream boundary is located in the solid nozzle region of the tunnel where the flow direction is constrained by the known wall slopes SLA and SLB. If this condition cannot be met or if other conditions, such as poor resolution of the wall pressures, prevent accurate modeling of this upstream region, SLA and SLB may be input as zero and the tunnel flow direction monitored by comparing the orientation of the airfoil shape calculated in the tunnel flow solution with the known incidence of the test airfoil. It has been observed that for supercritical cases, the calculated airfoil orientation is affected by the choice between conservative and nonconservative differencing at shock points. Because it is not yet clear which choice leads to the most accurate angle of attack correction, the choice is made optional as described in the following section.

Computational Control Inputs

The parameters discussed in this section affect the differencing form, convergence rate, stabilization, termination and amount of diagnostic output for the iterative process in each of the three solutions. Default values of each of these parameters are established in the program but may be overridden simply by including new values in the NPUT namelist.

The integer parameter ICNSV, if left as its default value of 1 provides for fully conservative differencing of the governing equation. Nonconservative differencing at shock points may be selected by setting ICNSV = 0.

The real parameter RFM affects only the model perturbation solution and is the underrelaxation factor used in transferring the Mach number correction evaluated at the match point to the far field. The default value of 0.2 is satisfactory for most cases but a smaller value might be needed to avoid oscillatory instability if the match point is located in or just upstream of a

very strong shock. The real parameter RFA, used only in the equivalent free air solution, similarly controls the angle of attack adjustment in response to a mismatch between the circulation integral around the airfoil and the circulation value prescribed for the far field and wake.

The five remaining parameters are dimensioned quantities denoting values stored in three-element arrays. The array subscripts from 1 to 3 correspond to the three successive flow solutions. The real array ORF contains the over-relaxation factor used at subsonic points in the successive line overrelaxation procedure. The real array DXT contains a damping factor to retard updating of longitudinal velocity perturbations. The real array EPS contains the convergence criterion in terms of the absolute value of the perturbation potential change in one iteration at the grid location where this change is greatest. Iteration is termined either when this criterion is met or when the number of iteration steps exceeds the value obtained from the integer array IMX. Information describing the convergence history is available for output at each step of iteration. The values stored in the integer array ITRC determine how much of this information is actually printed. An ITRC value of 1 causes printing at each iteration step; a value of 2 causes printing every tenth step and at termination; and the dafault value of zero causes only the final values to be printed so that it may be determined whether the iteration converged or ran the maximum number of steps. If either of the first two solutions is terminated by reaching the maximum number of iterations and the final value of the convergence parameter is greater than 10 times the criterion given in EPS, then all further processing of that case is aborted.

Pressure Distribution Inputs

In the tunnel flow computation, the outer boundary conditions are established from the input pressure coefficient distributions along or near the upper and lower tunnel walls. Similarly, the inner boundary conditions are established from input pressure coefficient distributions on the airfoil upper and lower surface. These data are input through parameters in the namelist block RDPX. The wall pressure data are described in a two-element integer array and two real two-dimensional arrays. The integers NW(1) and NW(2) are the numbers of pressure input locations along the upper and lower walls respectively. The first real array XW inputs the x coordinates of the wall pressure locations in order from upstream to downstream. The first index numbers these locations from 1 to the appropriate NW element and the second index is 1 or 2 for the upper or lower wall respectively. The second real array CPW inputs the pressure coefficients with the same order and indexing as their corresponding locations. The airfoil upper and lower surface pressure coefficients and their chordwise locations are input in a fully analogous manner using the integers NM(1), and NM(2) and the arrays XM and CPM. All four real arrays are dimensioned to accommodate values of NW or NM up to 30.

All input pressure distributions are interpolated onto boundary points located at the centers of the longitudinal mesh intervals. These boundary points range from J2 + 3/2 to J3 - 1/2 on the airfoil (K = 1) and from JU + 1/2 to JD - 1/2 on the outer boundary (K = KW). The interpolation routine

fits a spline to each distribution with a zero second derivative condition at the spline ends. Because the routine as presently implemented does not provide for extrapolation, each input pressure distribution must cover the full range of boundary points. Manual extrapolation of the experimental pressures at the airfoil trailing edge might be necessary in some cases to provide the required range of data. Near the leading edge, on the other hand, the number of experimental measurements might far exceed the requirements of this program and, therefore, one might omit some of the experimental data. Care should be taken not to introduce spurious oscillations in the spline fit between data points. One might even input a false pressure coefficient at the leading edge to help the spline provide a smooth fairing in the range of interest.

DESCRIPTION OF OUTPUT

Output is generated during each major phase of computation so that the user may scrutinize the processes leading to the final wall-induced perturbation results. The process output will be described in four sequential phases, input processing, tunnel flow solution, model perturbation solution, and equivalent free air solution. All output velocities are expressed in units of the reference stream velocity corresponding to the input tunnel Mach number AMREF. All output velocity potentials are expressed in units of the product of this reference velocity and the airfoil chord.

Input Processing

The contents of the namelist block NPUT are listed first. The longitudinal grid structure is then described by listing the x location and the derivative dJ/dx. These quantities evaluated at the grid lines J are identified as X(J) and F1(J). The corresponding quantities evaluated at J + 1/2 are given by XMID(J) and F2(J). The lateral grid structure is described by the grid line location Y(K), and the derivative dK/dy evaluated at the grid lines G1(K) and at the K + 1/2 points G2(K). The user should check to see that Y(KW) is the lateral location of the input wall pressures. The results of interpolating the airfoil pressure coefficients onto the mesh midpoints XMID(J) are then listed in separate groups for the upper and lower surfaces. This listing can be used in conjunction with the input data to judge the quality of the spline fit.

Tunnel Flow Solution

The convergence history of the tunnel flow solution is shown by listing the iteration number I, the largest change in the perturbation potential from the previous iteration DPHIMX, and the grid intersection JMX, KMX where this change is located. Negative values of KMX indicate points in the lower half plane. The flag ISUP is 1 if this grid point is a supersonic point and 0 if it is subsonic. The number of supersonic points NS and the current value of airfoil trailing edge thickness TTE are also listed. Both the inner and the outer boundary conditions depend on the solution and therefore are updated

iteratively. To avoid using poorly developed data for the update, it is performed only when the convergence parameter DPHIMX is less than some threshold value. The threshold levels specified for the inner and outer boundary condition updates are 10^{-3} and EPS(1)*10. respectively. The threshold levels are separated so that numerical problems associated with each update process might be identified more readily. Because the initial approximation to the inner boundary conditions is poor, it is normal for the convergence history to show that DPHIMX bounces up from the 10^{-3} level several times before sinking through it. This listing will end either with DPHIMX $\leq$ EPS(1) or with I = IMX(1) depending on whether or not convergence was achieved.

The data in the following listings are identified by a heading as pertinent to the tunnel flow. The critical pressure coefficient is given as CPSTAR. Data evaluated at the airfoil surface are listed next. Two lines are printed for each grid index J. Data on the first line pertain to the uppper surface or both surfaces and those on the second line to the lower surface or the increment between surfaces. The first four columns give data evaluated at the center of the mesh interval upstream from J. The calculated shape of the airfoil surface streamlines is given by the coordinates X(J-.5) and YMOD. The pressure coefficient CP(REF) can be compared with the previous listing of interpolated pressure coefficients to see how well the inner boundary conditions were satisfied. The longitudinal perturbation velocity component U is obtained directly from the potential gradient along the K = 1 grid line. The data in the last four columns are evaluated at the grid points located at X(J). V is the lateral component of perturbation velocity and DELTA PHI and DELTA V are the increments between the upper and lower surface values of the perturbation potential and the lateral velocity respectively. These increments are stored for use as the model boundary conditions in the model perturbation computation.

The perturbation velocity components along the outer boundaries of the tunnel flow computational region are given next. The next listing pertains to the upstream and downstream boundaries. The different coordinate locations given for the two components reflect the fact that U is evaluated over longitudinal mesh intervals and V over lateral mesh intervals. In the case of the upper and lower boundaries listed next, the V component is extrapolated to grid points on the K = KW boundary. Thus, the listed values of U and V are given at the indicated longitudinal location along the upper and lower boundaries at K = KW.

The final listing from the tunnel flow solution gives the perturbation potential at grid points in the immediate vicinity of the airfoil. The grid points are those on the K = 1, 2, and 3 grid lines in the upper and lower half planes for J from J1 to J4.

Model Perturbation Solution

Data output listed for the model perturbation solution is structured similarly to that described for the tunnel flow solution. This discussion, therefore, will highlight the differences between the two.

In the model perturbation solution, the far field Mach number is updated after each iteration cycle for which the convergence parameter DPHIMX is less than EPS(2)*10. As was previously indicated, the numerical stability of this update can be affected by the input parameters JP and RFM. The update stability characteristics can be judged from the convergence history by comparing the sign and magnitude of the UFAC changes immediately following two successive penetrations of the EPS(2)*10. threshold.

After convergence, the final far field Mach number is given as AMINF, the corresponding velocity as UINF/UREF and the dynamic pressure ratio as QFAC. This far field condition represents the corrected reference condition for the tunnel data. Accordingly, the model surface pressures listed as CP(INF) as well as the critical pressure CPSTAR are in the form of pressure coefficients based on the corrected reference. The change from CP(REF) in the tunnel flow to CP(INF) at the match point JP - 1/2 is due simply to this reference change but, at other locations, it is also influenced by nonuniformity of the wall-induced blockage velocity. Similarly, the airfoil shape given by YMOD, when compared with that in the tunnel flow, might show not only a different angle of attack due to wall-induced downwash, but also differences in mean camber shape due to nonuniformity of wall-induced downwash. It should be noted that the perturbation velocities and the perturbation potential in the free-air solution output are perturbations from a uniform flow at the far field velocity UINF. The velocity unit, however, is still the tunnel reference velocity UREF.

The wall-induced velocities are calculated as the difference between the perturbation velocities calculated at the same locations in the two flow solutions. This is performed in the present program only along the tunnel center line (K = 1) from JU to JD. The lateral velocities in the free air solution VF and due to the walls VW are listed at the grid point locations XV. The longitudinal velocity perturbations in the free air solution UF and due to the walls UW are given at the mesh center location XU. Over the model chord, values corresponding to both upper and lower surfaces are given. Although the wall-induced velocities should be identical on the two surfaces, some differences can appear in VW which reflect the accuracy with which the velocity jump boundary conditions are satisfied.

Equivalent Free Air Solution

The convergence history listing for the equivalent free air solution includes the current value of DA, the angle of attack correction in radians. This solution should converge in a relatively small number of iterations. If convergence difficulties are encountered, the iteration process can generally be stabilized by some combination of reduced RFA, reduced ORF(3), and increased DXT(3).

After convergence, the final value of the angle of attack correction is listed and results at the airfoil surface are given in the same form as those from the previous solutions. The airfoil shape described by YMOD should be the airfoil shape from the tunnel flow solution rotated through the angle of attack correction. The numerical procedure used, however, applies the angle of attack

correction as a surface slope increment and the rotation is approximated by a shearing transformation. The listing of CP(INF) from the equivalent free air solution gives a pressure distribution in the form of coefficients based on the corrected free stream conditions and is, of course, free of the influence of any nonuniformity in the wall-induced velocity perturbation.

The final output gives the corrected lift coefficient and lists the result of transforming the experimental airfoil pressures to coefficients based on the corrected free stream conditions. The effect of any nonuniformity in the wall-induced velocity perturbations can be seen by comparing this distribution with the one resulting from the equivalent free air solution.

APPENDIX

SAMPLE CASE

The sample case consists of the application of program TWINTAN to a test case which was provided by M. Mokry and L. H. Ohman of the National Aeronautical Establishment, Ottawa, Ontario, Canada and has been used by them to compare several methods for interference corrections. The experimental data were obtained in a test of the BGK-1 airfoil in the NAE blowdown wind tunnel with 20 percent porosity top and bottom walls. The ratio of tunnel height to airfoil chord was 6. The airfoil was set at 2.56° incidence and tested at a reference Mach number of 0.784 and a Reynolds number of 21.03×10^6.

The input card images are listed and followed by the program output listing. The results of the model perturbation solution give a corrected Mach number of about 0.767 and show distributions of the wall-induced velocities VW and UW which are nearly uniform over the model chord. The results of the equivalent free air solution indicate an angle of attack correction of about -0.0112 radians which corresponds to -0.64°. If, however, the airfoil shape calculated in the tunnel flow solution is plotted and compared with the actual BGK-1 airfoil shape at 2.56° incidence, it is found that the correspondence between shapes is improved by adding downwash to the tunnel flow solution equivalent to a rotation of 0.25°. The corresponding angle of attack correction would then be -0.89°.

INPUT FOR SAMPLE CASE

```
$NPUT J1=29,J3=51,J4=53,J5=75,M=34,DXMN=.0488,JU=1,JD=75,KB=23,N=30,
DYMN=.048333,KW=21,
AMREF=.784,CL=.764,CD=.03,SLA=0.,SLB=0.,JP=44,
ICNSV=0,OPF(1)=2*1.85,ITRC(1)=2,2,1$
$RDPX NW(1)=15,14,XW(1,1)=-7.85,-5.75,-3.35,-2.15,-1.25,-.65,.1,.7,1.15,
1.6,2.35,2.95,3.55,4.15,4.75,XW(1,2)=-7.85,-5.75,-3.35,-2.15,-1.25,-.65,
.1,.7,1.3,1.75,2.35,2.95,4.15,4.75,NM(1)=24,14,XM(1,1)=.025,.0402,.0602,
.08015,.1002,.14,.2,.26,.3402,.4004,.4402,.5004,.56045,.58035,.6002,.6201,
.6501,.7001,.7503,.8003,.8502,.9004,.95,1.,XM(1,2)=.0198,.05,.1003,.1504,.2001,
.2501,.3496,.4501,.5504,.65035,.7503,.8497,.95,1.,
CPW(1,1)=-.0063,-.0013,.0135,.0191,.0064,-.0049,-.0212,-.0277,-.0242,-.0245,
-.0274,-.0232,-.0196,-.0172,-.0172,CPW(1,2)=-.0064,.01,.029,.0422,.0553,
.0721,.0842,.0944,.0949,.0905,.0797,.0688,.0396,.0257,CPM(1,1)=-.4455,
-.5856,-.7686,-.9334,-.9919,-1.0309,-1.0327,-1.0446,-1.0476,-1.0623,-1.0828,
-1.112,-1.1347,-1.1416,-1.1343,-.8942,-.5369,-.3707,-.2454,-.1454,-.044,.0496,
.1344,.224,CPM(1,2)=.4226,.1443,-.0498,-.1415,-.1906,-.2088,-.2049,-.1172,
-.0072,.1695,.3345,.4078,.3795,.224$
```

SAMPLE CASE OUTPUT

```
$NPUT
J1      = 29,
J3      = 51,
J4      = 53,
J5      = 75,
M       = 34,
DXMN    = .488E-01,
JU      = 1,
JD      = 75,
KB      = 23,
N       = 30,
DYMN    = .48333E-01,
KW      = 21,
AMREF   = .784E+00,
CL      = .764E+00,
CD      = .3E-01,
SLA     = 0.0,
SLB     = 0.0,
JP      = 44,
ICNSV   = 0,
RFM     = .2E+00,
RFA     = .5E+00,
DRF     = .185E+01, .185E+01, .18E+01,
DXT     = .5E+00, .5E+00, .5E+00,
ITRC    = 2, 2, 1,
EPS     = .5E-05, .5E-05, .5E-05,
IMX     = 350, 500, 200,
$END
```

J	X(J)	F1(J)	F2(J)	XMID(J)
1	-.78165E+01	.63815E+00	.74894E+00	-.71489E+01
2	-.64734E+01	.86860E+00	.99711E+00	-.59719E+01
3	-.54660E+01	.11345E+01	.12807E+01	-.50756E+01
4	-.46825E+01	.14358E+01	.15998E+01	-.43700E+01
5	-.40557E+01	.17726E+01	.19543E+01	-.37998E+01
6	-.35428E+01	.21449E+01	.23443E+01	-.33296E+01
7	-.31155E+01	.25526E+01	.27698E+01	-.29349E+01
8	-.27538E+01	.29958E+01	.32306E+01	-.25991E+01
9	-.24439E+01	.34744E+01	.37270E+01	-.23097E+01
10	-.21753E+01	.39885E+01	.42588E+01	-.20578E+01
11	-.19402E+01	.45380E+01	.48260E+01	-.18366E+01
12	-.17328E+01	.51230E+01	.54287E+01	-.16407E+01
13	-.15484E+01	.57434E+01	.60669E+01	-.14660E+01
14	-.13835E+01	.63993E+01	.67405E+01	-.13093E+01
15	-.12350E+01	.70906E+01	.74496E+01	-.11679E+01
16	-.11007E+01	.78174E+01	.81941E+01	-.10397E+01
17	-.97862E+00	.85796E+01	.89740E+01	-.92290E+00
18	-.86713E+00	.93773E+01	.97894E+01	-.81606E+00
19	-.76493E+00	.10210E+02	.10640E+02	-.71794E+00
20	-.67091E+00	.11079E+02	.11527E+02	-.62753E+00
21	-.58412E+00	.11983E+02	.12448E+02	-.54396E+00
22	-.50376E+00	.12923E+02	.13406E+02	-.46647E+00
23	-.42914E+00	.13898E+02	.14398E+02	-.39442E+00
24	-.35967E+00	.14908E+02	.15426E+02	-.32726E+00
25	-.29483E+00	.15954E+02	.16490E+02	-.26451E+00
26	-.23417E+00	.17035E+02	.17589E+02	-.20574E+00
27	-.17730E+00	.18152E+02	.18724E+02	-.15060E+00
28	-.12388E+00	.19304E+02	.19894E+02	-.98745E-01
29	-.73600E-01	.20492E+02	.20492E+02	-.49200E-01
30	-.24800E-01	.20492E+02	.20492E+02	-.40000E-03
31	.24000E-01	.20492E+02	.20492E+02	.48400E-01
32	.72800E-01	.20492E+02	.20492E+02	.97200E-01
33	.12160E+00	.20492E+02	.20492E+02	.14600E+00
34	.17040E+00	.20492E+02	.20492E+02	.19480E+00
35	.21920E+00	.20492E+02	.20492E+02	.24360E+00
36	.26800E+00	.20492E+02	.20492E+02	.29240E+00
37	.31680E+00	.20492E+02	.20492E+02	.34120E+00
38	.36560E+00	.20492E+02	.20492E+02	.39000E+00
39	.41440E+00	.20492E+02	.20492E+02	.43880E+00
40	.46320E+00	.20492E+02	.20492E+02	.48760E+00
41	.51200E+00	.20492E+02	.20492E+02	.53640E+00
42	.56080E+00	.20492E+02	.20492E+02	.58520E+00
43	.60960E+00	.20492E+02	.20492E+02	.63400E+00
44	.65840E+00	.20492E+02	.20492E+02	.68280E+00
45	.70720E+00	.20492E+02	.20492E+02	.73160E+00
46	.75600E+00	.20492E+02	.20492E+02	.78040E+00
47	.80480E+00	.20492E+02	.20492E+02	.82920E+00
48	.85360E+00	.20492E+02	.20492E+02	.87800E+00
49	.90240E+00	.20492E+02	.20492E+02	.92680E+00
50	.95120E+00	.20492E+02	.20492E+02	.97560E+00

51	.10000E+01	.20492E+02	.20492E+02	.10244E+01
52	.10488E+01	.20492E+02	.20492E+02	.10732E+01
53	.10976E+01	.20492E+02	.19894E+02	.11227E+01
54	.11479E+01	.19304E+02	.18724E+02	.11746E+01
55	.12013E+01	.18152E+02	.17589E+02	.12297E+01
56	.12582E+01	.17035E+02	.16490E+02	.12885E+01
57	.13188E+01	.15954E+02	.15426E+02	.13512E+01
58	.13837E+01	.14908E+02	.14398E+02	.14184E+01
59	.14531E+01	.13898E+02	.13406E+02	.14904E+01
60	.15278E+01	.12923E+02	.12448E+02	.15679E+01
61	.16081E+01	.11983E+02	.11527E+02	.16515E+01
62	.16949E+01	.11079E+02	.10640E+02	.17419E+01
63	.17889E+01	.10210E+02	.97894E+01	.18400E+01
64	.18911E+01	.93773E+01	.89740E+01	.19468E+01
65	.20026E+01	.85796E+01	.81941E+01	.20636E+01
66	.21247E+01	.78174E+01	.74496E+01	.21918E+01
67	.22590E+01	.70906E+01	.67405E+01	.23332E+01
68	.24075E+01	.63993E+01	.60669E+01	.24899E+01
69	.25724E+01	.57434E+01	.54287E+01	.26645E+01
70	.27568E+01	.51230E+01	.48260E+01	.28604E+01
71	.29642E+01	.45380E+01	.42588E+01	.30816E+01
72	.31993E+01	.39885E+01	.37270E+01	.33334E+01
73	.34679E+01	.34744E+01	.32306E+01	.36227E+01
74	.37778E+01	.29958E+01	.27698E+01	.39584E+01
75	.41395E+01	.25526E+01	.23443E+01	.43527E+01

K	Y(K)	G1(K)	G2(K)
1	0.	.20690E+02	.20006E+02
2	.50000E-01	.19333E+02	.18673E+02
3	.10357E+00	.18023E+02	.17385E+02
4	.16111E+00	.16759E+02	.16144E+02
5	.22308E+00	.15540E+02	.14948E+02
6	.29000E+00	.14368E+02	.13799E+02
7	.36250E+00	.13241E+02	.12695E+02
8	.44130E+00	.12161E+02	.11638E+02
9	.52727E+00	.11127E+02	.10627E+02
10	.62142E+00	.10138E+02	.96610E+01
11	.72500E+00	.91955E+01	.87414E+01
12	.83947E+00	.82989E+01	.78679E+01
13	.96666E+00	.74483E+01	.70403E+01
14	.11088E+01	.66437E+01	.62587E+01
15	.12687E+01	.58851E+01	.55230E+01
16	.14500E+01	.51724E+01	.48334E+01
17	.16571E+01	.45058E+01	.41897E+01
18	.18961E+01	.38851E+01	.35920E+01
19	.21750E+01	.33104E+01	.30403E+01
20	.25045E+01	.27816E+01	.25345E+01
21	.29000E+01	.22989E+01	.20747E+01
22	.33833E+01	.18621E+01	.16609E+01
23	.39875E+01	.14713E+01	.12931E+01

AIRFOIL CP INTERPOLATED AT MESH MIDPOINTS

-.66018	-.98743	-1.03323	-1.03281	-1.04092	-1.04717	-1.04767	-1.05809	-1.08208	-1.10536
-1.13080	-1.15017	-.70513	-.39726	-.29534	-.18227	-.08718	.00947	.09477	.17975
.15611	-.04324	-.13498	-.18724	-.20728	-.21550	-.20857	-.17643	-.12863	-.08033
-.02606	.04798	.13809	.23050	.31041	.36387	.39603	.42325	.41531	.30876

I	JMX	KMX	ISUP	NS	DPHIMX	TTE
10	58	-1	0	83	.14972E+00	0.
20	59	-1	0	98	.32637E-01	0.
30	60	-1	0	104	.57918E-02	0.
40	43	10	0	88	.28225E-02	0.
50	27	-12	0	94	-.10169E-02	0.
60	31	3	0	97	-.23619E-02	-.10111E+00
70	31	3	0	96	-.10462E-02	-.10111E+00
80	31	3	0	95	-.99001E-03	-.40739E-01
90	29	1	0	95	-.10775E-02	-.36273E-03
100	29	1	0	94	-.69197E-03	.16329E-01
110	22	-9	0	96	-.35498E-03	.14887E-01
120	28	-10	0	96	-.19063E-03	.15835E-01
130	25	-13	0	96	-.94511E-04	.15230E-01
140	25	-11	0	96	-.47021E-04	.15148E-01
150	66	-3	0	96	-.13578E-03	.15088E-01
160	57	8	0	96	-.42739E-04	.14991E-01
170	47	-10	0	96	-.23393E-04	.14965E-01
180	38	-14	0	96	-.12391E-04	.15014E-01
190	29	-15	0	96	-.62766E-05	.15024E-01
195	24	-13	0	96	-.48187E-05	.15020E-01

PESULTS IN TUNNEL FLOW

CPSTAR = -.48183E+00

X(J-.5)	YMOD	CP(REF)	U	J	X(J)	V	DELTA PHI	DELTA V
-.00040	0.00000	.81668	-.44457	31	.02400	.64698		
	0.00000	1.04505	-.69171			-.61341	.01206	1.26040
.04840	.03157	-.65531	.43819	32	.07280	.23048		
	-.02993	.14630	.00250			-.21816	.03332	.44863
.09720	.04282	-.98835	.50106	33	.12160	.10789		
	-.04058	-.04325	.03945			-.15799	.05585	.26588
.14600	.04808	-1.03534	.50885	34	.17040	.05745		
	-.04829	-.13500	.07642			-.11232	.07695	.16978
.19480	.05089	-1.03288	.50379	35	.21920	.02607		
	-.05377	-.18725	.09705			-.07635	.09680	.10242
.24360	.05216	-1.04089	.50665	36	.26800	-.00159		
	-.05750	-.20729	.10406			-.04819	.11645	.04660
.29240	.05208	-1.04715	.50982	37	.31680	-.02213		
	-.05985	-.21550	.10660			-.02228	.13612	.00015
.34120	.05100	-1.04768	.51066	38	.36560	-.03753		
	-.06094	-.20857	.10260			.00332	.15604	-.04085
.39000	.04917	-1.05821	.51697	39	.41440	-.05530		
	-.06077	-.17643	.08705			.02563	.17702	-.08093
.43880	.04647	-1.08205	.53085	40	.46320	-.07704		
	-.05952	-.12863	.06424			.04327	.19979	-.12031
.48760	.04271	-1.10508	.54521	41	.51200	-.09771		
	-.05741	-.08033	.04126			.05997	.22438	-.15769
.53640	.03795	-1.13017	.56146	42	.56080	-.11982		
	-.05449	-.02606	.01540			.07776	.25103	-.19758
.58520	.03210	-1.14320	.57180	43	.60960	-.13630		
	-.05069	.04798	-.02060			.09196	.27994	-.22827
.63400	.02545	-.70622	.34367	44	.65840	.02360		
	-.04620	.13808	-.06594			.09698	.29993	-.07338
.68280	.02660	-.40090	.19637	45	.70720	-.11440		
	-.04147	.23046	-.11457			.08910	.31510	-.20350
.73160	.02102	-.29546	.15453	46	.75600	-.15059		
	-.03712	.31037	-.15875			.06730	.33039	-.21790
.78040	.01367	-.18235	.10348	47	.80480	-.16715		
	-.03384	.36385	-.18963			.03916	.34469	-.20631
.82920	.00551	-.08720	.05860	48	.85360	-.17707		
	-.03193	.39602	-.20857			.01038	.35773	-.18744
.87800	-.00313	.00947	.01076	49	.90240	-.17726		
	-.03142	.42325	-.22424			-.03276	.36920	-.14450
.92680	-.01178	.09476	-.03350	50	.95120	-.17127		
	-.03302	.41527	-.21831			-.08807	.37822	-.08320
.97560	-.02014	.17971	-.07975	51	1.00000	-.15391		
	-.03732	.30869	-.15728			-.08451	.38200	-.06940
1.02440	-.02765							
	-.04144							

OUTER BOUNDARY VELOCITIES

		X =	-.71489E+01	-.78165E+01	.39584E+01	.41395E+01
YU	YV		U	V	U	V
0.	.24993E-01		-.14172E-02	.63647E-03	-.71975E-02	-.14018E-01
.50000E-01	.76777E-01		-.13974E-02	.61360E-03	-.69205E-02	-.14145E-01
.10357E+00	.13233E+00		-.13740E-02	.58868E-03	-.66230E-02	-.14277E-01
.16111E+00	.19208E+00		-.13463E-02	.56150E-03	-.63027E-02	-.14415E-01
.22308E+00	.25652E+00		-.13136E-02	.53180E-03	-.59569E-02	-.14559E-01
.29000E+00	.32623E+00		-.12749E-02	.49932E-03	-.55827E-02	-.14710E-01
.36250E+00	.40188E+00		-.12291E-02	.46380E-03	-.51764E-02	-.14867E-01
.44130E+00	.48426E+00		-.11745E-02	.42492E-03	-.47340E-02	-.15030E-01
.52727E+00	.57432E+00		-.11096E-02	.38240E-03	-.42507E-02	-.15200E-01
.62142E+00	.67318E+00		-.10320E-02	.33595E-03	-.37208E-02	-.15375E-01
.72500E+00	.78219E+00		-.93881E-03	.28537E-03	-.31378E-02	-.15555E-01
.83947E+00	.90302E+00		-.82653E-03	.23056E-03	-.24937E-02	-.15739E-01
.96666E+00	.10377E+01		-.69052E-03	.17167E-03	-.17791E-02	-.15923E-01
.11088E+01	.11887E+01		-.52485E-03	.10928E-03	-.98259E-03	-.16105E-01
.12687E+01	.13593E+01		-.32181E-03	.44796E-04	-.90493E-04	-.16278E-01
.14500E+01	.15534E+01		-.71363E-04	-.19009E-04	.91422E-03	-.16434E-01
.16571E+01	.17765E+01		.23966E-03	-.76823E-04	.20529E-02	-.16559E-01
.18961E+01	.20353E+01		.62847E-03	-.11876E-03	.33530E-02	-.16632E-01
.21750E+01	.23394E+01		.11173E-02	-.12641E-03	.48523E-02	-.16616E-01
.25045E+01	.27018E+01		.17335E-02	-.65014E-04	.66061E-02	-.16456E-01
0.	-.24993E-01		-.14172E-02	.65818E-03	-.71975E-02	-.13894E-01
-.50000E-01	-.76777E-01		-.14351E-02	.68026E-03	-.74743E-02	-.13762E-01
-.10357E+00	-.13233E+00		-.14520E-02	.70341E-03	-.77700E-02	-.13617E-01
-.16111E+00	-.19208E+00		-.14677E-02	.72764E-03	-.80866E-02	-.13456E-01
-.22308E+00	-.25652E+00		-.14816E-02	.75292E-03	-.84262E-02	-.13279E-01
-.29000E+00	-.32623E+00		-.14933E-02	.77916E-03	-.87913E-02	-.13082E-01
-.36250E+00	-.40188E+00		-.15020E-02	.80624E-03	-.91850E-02	-.12861E-01
-.44130E+00	-.48426E+00		-.15068E-02	.83391E-03	-.96105E-02	-.12614E-01
-.52727E+00	-.57432E+00		-.15065E-02	.86179E-03	-.10072E-01	-.12334E-01
-.62142E+00	-.67318E+00		-.14997E-02	.88929E-03	-.10574E-01	-.12016E-01
-.72500E+00	-.78219E+00		-.14844E-02	.91548E-03	-.11121E-01	-.11652E-01
-.83947E+00	-.90302E+00		-.14582E-02	.93897E-03	-.11722E-01	-.11232E-01
-.96666E+00	-.10377E+01		-.14177E-02	.95765E-03	-.12382E-01	-.10744E-01
-.11088E+01	-.11887E+01		-.13586E-02	.96827E-03	-.13113E-01	-.10171E-01
-.12687E+01	-.13593E+01		-.12753E-02	.96582E-03	-.13928E-01	-.94920E-02
-.14500E+01	-.15534E+01		-.11602E-02	.94248E-03	-.14842E-01	-.86774E-02
-.16571E+01	-.17765E+01		-.10033E-02	.88578E-03	-.15880E-01	-.76869E-02
-.18961E+01	-.20353E+01		-.79135E-03	.77547E-03	-.17074E-01	-.64636E-02
-.21750E+01	-.23394E+01		-.50690E-03	.57767E-03	-.18475E-01	-.49254E-02
-.25045E+01	-.27018E+01		-.12816E-03	.23388E-03	-.20168E-01	-.29493E-02

		Y =	.29000E+01	.29000E+01	-.29000E+01	-.29000E+01
XU	XV		U	V	U	V
-.71489E+01	-.78165E+01		.25072E-02		.36941E-03	
-.59719E+01	-.64734E+01		.10247E-02	.26550E-02	-.41939E-02	-.17655E-02
-.50756E+01	-.54660E+01		-.80003E-03	.46979E-02	-.73929E-02	-.16798E-02
-.43700E+01	-.46825E+01		-.28168E-02	.64776E-02	-.99856E-02	-.14948E-02
-.37998E+01	-.40557E+01		-.48768E-02	.79912E-02	-.12365E-01	-.14866E-02
-.33296E+01	-.35428E+01		-.68958E-02	.92090E-02	-.14649E-01	-.16209E-02
-.29349E+01	-.31155E+01		-.86739E-02	.10031E-01	-.16818E-01	-.18286E-02
-.25991E+01	-.27538E+01		-.97369E-02	.10334E-01	-.18734E-01	-.20503E-02
-.23097E+01	-.24439E+01		-.99262E-02	.10313E-01	-.20346E-01	-.23374E-02
-.20578E+01	-.21753E+01		-.92929E-02	.10189E-01	-.21663E-01	-.27598E-02
-.18366E+01	-.19402E+01		-.80934E-02	.10179E-01	-.22837E-01	-.34230E-02
-.16407E+01	-.17328E+01		-.66636E-02	.10391E-01	-.24080E-01	-.43724E-02
-.14660E+01	-.15484E+01		-.52005E-02	.10758E-01	-.25495E-01	-.55152E-02
-.13093E+01	-.13835E+01		-.38100E-02	.11193E-01	-.27112E-01	-.67484E-02
-.11679E+01	-.12350E+01		-.25427E-02	.11614E-01	-.28919E-01	-.79746E-02
-.10397E+01	-.11007E+01		-.13881E-02	.11936E-01	-.30787E-01	-.90428E-02
-.92290E+00	-.97862E+00		-.31399E-03	.12113E-01	-.32560E-01	-.98811E-02
-.81606E+00	-.86713E+00		.70150E-03	.12131E-01	-.34151E-01	-.10519E-01
-.71794E+00	-.76493E+00		.16726E-02	.11994E-01	-.35515E-01	-.10996E-01
-.62753E+00	-.67091E+00		.26084E-02	.11707E-01	-.36636E-01	-.11353E-01
-.54396E+00	-.58412E+00		.35100E-02	.11288E-01	-.37534E-01	-.11649E-01
-.46647E+00	-.50376E+00		.43696E-02	.10757E-01	-.38267E-01	-.11951E-01
-.39442E+00	-.42914E+00		.51821E-02	.10127E-01	-.38879E-01	-.12268E-01
-.32726E+00	-.35967E+00		.59454E-02	.94061E-02	-.39404E-01	-.12599E-01
-.26451E+00	-.29483E+00		.66588E-02	.86069E-02	-.39867E-01	-.12939E-01
-.20574E+00	-.23417E+00		.73233E-02	.77402E-02	-.40287E-01	-.13284E-01
-.15060E+00	-.17730E+00		.79403E-02	.68173E-02	-.40675E-01	-.13630E-01
-.98745E-01	-.12388E+00		.85118E-02	.58492E-02	-.41043E-01	-.13971E-01
-.49200E-01	-.73600E-01		.90477E-02	.48348E-02	-.41402E-01	-.14316E-01
-.40000E-03	-.24800E-01		.95635E-02	.37915E-02	-.41768E-01	-.14641E-01
.48400E-01	.24000E-01		.10065E-01	.26525E-02	-.42151E-01	-.14984E-01
.97200E-01	.72800E-01		.10550E-01	.14334E-02	-.42557E-01	-.15332E-01
.14600E+00	.12160E+00		.11017E-01	.13883E-03	-.42989E-01	-.15678E-01
.19480E+00	.17040E+00		.11460E-01	-.12230E-02	-.43442E-01	-.16005E-01
.24360E+00	.21920E+00		.11876E-01	-.26438E-02	-.43910E-01	-.16304E-01
.29240E+00	.26800E+00		.12260E-01	-.41145E-02	-.44386E-01	-.16574E-01

.34120E+00	.31680E+00	.12608E-01	-.56246E-02	-.44865E-01	-.16811E-01
.39000E+00	.36560E+00	.12916E-01	-.71620E-02	-.45338E-01	-.17014E-01
.43880E+00	.41440E+00	.13179E-01	-.87140E-02	-.45801E-01	-.17183E-01
.48760E+00	.46320E+00	.13393E-01	-.10267E-01	-.46246E-01	-.17316E-01
.53640E+00	.51200E+00	.13555E-01	-.11807E-01	-.46667E-01	-.17413E-01
.58520E+00	.56080E+00	.13660E-01	-.13322E-01	-.47057E-01	-.17475E-01
.63400E+00	.60960E+00	.13705E-01	-.14798E-01	-.47411E-01	-.17504E-01
.68280E+00	.65840E+00	.13686E-01	-.16226E-01	-.47720E-01	-.17499E-01
.73160E+00	.70720E+00	.13599E-01	-.17599E-01	-.47980E-01	-.17464E-01
.78040E+00	.75600E+00	.13451E-01	-.18923E-01	-.48190E-01	-.17412E-01
.82920E+00	.80480E+00	.13255E-01	-.20205E-01	-.48352E-01	-.17352E-01
.87800E+00	.85360E+00	.13024E-01	-.21440E-01	-.48470E-01	-.17285E-01
.92680E+00	.90240E+00	.12770E-01	-.22627E-01	-.48547E-01	-.17214E-01
.97560E+00	.95120E+00	.12507E-01	-.23762E-01	-.48584E-01	-.17139E-01
.10244E+01	.10000E+01	.12247E-01	-.24844E-01	-.48586E-01	-.17062E-01
.10732E+01	.10488E+01	.12003E-01	-.25871E-01	-.48556E-01	-.16984E-01
.11227E+01	.10976E+01	.11785E-01	-.26839E-01	-.48495E-01	-.16901E-01
.11746E+01	.11479E+01	.11603E-01	-.27789E-01	-.48401E-01	-.16817E-01
.12297E+01	.12013E+01	.11468E-01	-.28711E-01	-.48272E-01	-.16725E-01
.12885E+01	.12582E+01	.11384E-01	-.29582E-01	-.48106E-01	-.16623E-01
.13512E+01	.13188E+01	.11356E-01	-.30385E-01	-.47902E-01	-.16509E-01
.14184E+01	.13837E+01	.11387E-01	-.31100E-01	-.47651E-01	-.16368E-01
.14904E+01	.14531E+01	.11478E-01	-.31709E-01	-.47341E-01	-.16189E-01
.15679E+01	.15270E+01	.11631E-01	-.32188E-01	-.46955E-01	-.15965E-01
.16515E+01	.16081E+01	.11840E-01	-.32514E-01	-.46473E-01	-.15686E-01
.17419E+01	.16949E+01	.12099E-01	-.32664E-01	-.45867E-01	-.15342E-01
.18400E+01	.17889E+01	.12396E-01	-.32613E-01	-.45105E-01	-.14930E-01
.19468E+01	.18911E+01	.12710E-01	-.32333E-01	-.44173E-01	-.14471E-01
.20636E+01	.20026E+01	.13004E-01	-.31796E-01	-.43071E-01	-.13975E-01
.21918E+01	.21247E+01	.13219E-01	-.30977E-01	-.41812E-01	-.13445E-01
.23332E+01	.22590E+01	.13260E-01	-.29854E-01	-.40432E-01	-.12881E-01
.24899E+01	.24075E+01	.13004E-01	-.28438E-01	-.38979E-01	-.12258E-01
.26645E+01	.25724E+01	.12436E-01	-.26845E-01	-.37409E-01	-.11463E-01
.28604E+01	.27568E+01	.11644E-01	-.25185E-01	-.35587E-01	-.10401E-01
.30816E+01	.29642E+01	.10832E-01	-.23542E-01	-.33289E-01	-.90154E-02
.33334E+01	.31993E+01	.10115E-01	-.21873E-01	-.30334E-01	-.73698E-02
.36227E+01	.34679E+01	.94160E-02	-.20085E-01	-.26665E-01	-.55885E-02
.39584E+01	.37778E+01	.87079E-02	-.18217E-01	-.22303E-01	-.37565E-02

PHI IN VICINITY OF AIRFOIL

J	PHI(J,3,2)	PHI(J,2,2)	PHI(J,1,2)	PHI(J,1,1)	PHI(J,2,1)	PHI(J,3,1)
29	-.14693E+00	-.14677E+00	-.14428E+00	-.14428E+00	-.13808E+00	-.13021E+00
30	-.15732E+00	-.16010E+00	-.15975E+00	-.15975E+00	-.14830E+00	-.13661E+00
31	-.16795E+00	-.17693E+00	-.19351E+00	-.18145E+00	-.15778E+00	-.14087E+00
32	-.17422E+00	-.18281E+00	-.19339E+00	-.16007E+00	-.14855E+00	-.13620E+00
33	-.17683E+00	-.18384E+00	-.19146E+00	-.13561E+00	-.12948E+00	-.12171E+00
34	-.17690E+00	-.18225E+00	-.18773E+00	-.11078E+00	-.10780E+00	-.10352E+00
35	-.17539E+00	-.17922E+00	-.18300E+00	-.86198E-01	-.84965E-01	-.83047E-01
36	-.17303E+00	-.17552E+00	-.17792E+00	-.61473E-01	-.61513E-01	-.61214E-01
37	-.17032E+00	-.17158E+00	-.17272E+00	-.36594E-01	-.37656E-01	-.38556E-01
38	-.16767E+00	-.16778E+00	-.16771E+00	-.11674E-01	-.13538E-01	-.15379E-01
39	-.16547E+00	-.16459E+00	-.16346E+00	.13554E-01	.10880E-01	.82011E-02
40	-.16404E+00	-.16231E+00	-.16033E+00	.39460E-01	.35815E-01	.32240E-01
41	-.16353E+00	-.16109E+00	-.15831E+00	.66066E-01	.61406E-01	.56854E-01
42	-.16415E+00	-.16110E+00	-.15756E+00	.93465E-01	.87744E-01	.82144E-01
43	-.16607E+00	-.16265E+00	-.15857E+00	.12137E+00	.11473E+00	.10811E+00
44	-.16944E+00	-.16601E+00	-.16179E+00	.13814E+00	.13677E+00	.13217E+00
45	-.17423E+00	-.17119E+00	-.16738E+00	.14772E+00	.14211E+00	.13598E+00
46	-.18026E+00	-.17801E+00	-.17512E+00	.15526E+00	.14797E+00	.14057E+00
47	-.18724E+00	-.18603E+00	-.18438E+00	.16031E+00	.15225E+00	.14421E+00
48	-.19481E+00	-.19481E+00	-.19456E+00	.16317E+00	.15472E+00	.14642E+00
49	-.20260E+00	-.20396E+00	-.20550E+00	.16370E+00	.15529E+00	.14710E+00
50	-.21010E+00	-.21273E+00	-.21615E+00	.16206E+00	.15405E+00	.14633E+00
51	-.21678E+00	-.22003E+00	-.22383E+00	.15817E+00	.15113E+00	.14430E+00
52	-.22255E+00	-.22609E+00	-.23010E+00	.15190E+00	.14696E+00	.14143E+00
53	-.22744E+00	-.23094E+00	-.23466E+00	.14734E+00	.14320E+00	.13850E+00

I	JMX	KMX	ISUP	NS	DPHIMX	UFAC
10	68	-13	0	108	.18612E-01	0.
20	59	-10	0	109	.67615E-02	0.
30	49	-9	0	123	.35451E-02	0.
40	45	2	1	136	.22124E-02	0.
50	31	-14	0	136	.11244E-02	0.
60	22	-15	0	136	.74607E-03	0.
70	31	1	0	136	.52888E-03	0.
80	31	1	0	136	.39228E-03	0.
90	31	1	0	135	.30070E-03	0.
100	31	1	0	135	.22584E-03	0.
110	31	1	0	134	.16935E-03	0.
120	31	1	0	134	.12720E-03	0.
130	31	1	0	134	.95640E-04	0.
140	31	1	0	134	.72079E-04	0.
150	31	1	0	134	.54323E-04	0.
160	46	3	0	116	.33826E-02	.98176E+00
170	32	3	0	114	.30474E-03	.98176E+00
180	22	3	0	112	.17189E-03	.98176E+00
190	28	3	0	112	.81272E-04	.98176E+00
200	37	8	1	112	.69777E-04	.98136E+00
210	39	7	1	111	.52532E-04	.98091E+00
220	27	2	0	111	.30374E-04	.98093E+00
230	25	-3	0	111	.19915E-04	.98103E+00
240	27	-6	0	111	.13692E-04	.98107E+00
250	28	-7	0	111	.99122E-05	.98110E+00
260	28	-7	0	111	.73158E-05	.98112E+00
270	28	-6	0	111	.54218E-05	.98113E+00
273	28	-6	0	111	.49535E-05	.98113E+00

MODEL PERTURBATION (U AND V ARE PERTURBATIONS FROM UINF BUT NORMALIZED BY UREF)

JP = 44, AMINF = .76745, UINF/UREF = .98113, CPSTAR = -.53345E+00, QFAC = .97372

X(J-.5)	YMOD	CP(INF)	U	J	X(J)	V	DELTA PHI	DELTA V
-.00040	0.00000	.80657	-.42744	31	.02400	.65838		
	0.00000	1.03564	-.67458			-.60217	.01206	1.26054
.04840	.03213	-.68965	.45648	32	.07280	.24158		
	-.02939	.11051	.02079			-.20711	.03332	.44870
.09720	.04392	-1.04515	.51950	33	.12160	.11919		
	-.03949	-.08506	.05788			-.14675	.05585	.26594
.14600	.04973	-1.09732	.52721	34	.17040	.06880		
	-.04665	-.17875	.09478			-.10103	.07695	.16983
.19480	.05309	-1.09649	.52212	35	.21920	.03744		
	-.05158	-.23178	.11538			-.06503	.09680	.10247
.24360	.05492	-1.10594	.52502	36	.26800	.00981		
	-.05476	-.25182	.12244			-.03684	.11645	.04665
.29240	.05540	-1.11334	.52624	37	.31680	-.01070		
	-.05656	-.25974	.12502			-.01090	.13612	.00020
.34120	.05488	-1.11461	.52914	38	.36560	-.02608		
	-.05709	-.25209	.12108			.01471	.15604	-.04060
.39000	.05360	-1.12612	.53553	39	.41440	-.04382		
	-.05637	-.21860	.10561			.03706	.17702	-.08088
.43880	.05146	-1.15136	.54950	40	.46320	-.06552		
	-.05456	-.16913	.08288			.05473	.19979	-.12025
.48760	.04827	-1.17575	.56392	41	.51200	-.08614		
	-.05189	-.11920	.05998			.07149	.22438	-.15763
.53640	.04406	-1.20219	.58023	42	.56080	-.10817		
	-.04840	-.06314	.03418			.08936	.25103	-.19753
.58520	.03879	-1.21611	.59062	43	.60960	-.12456		
	-.04404	.01320	-.00178			.10365	.27994	-.22821
.63400	.03271	-.76546	.36253	44	.65840	.03544		
	-.03898	.10576	-.04708			.10876	.29993	-.07332
.68280	.03444	-.45206	.21549	45	.70720	-.10174		
	-.03368	.19998	-.09544			.10166	.31510	-.20340
.73160	.02947	-.34401	.17282	46	.75600	-.13789		
	-.02871	.28313	-.14046			.07990	.33039	-.21779
.78040	.02274	-.22692	.12122	47	.80480	-.15458		
	-.02482	.33837	-.17189			.05161	.34469	-.20619
.82920	.01520	-.12857	.07604	48	.85360	-.16466		
	-.02230	.37128	-.19113			.02267	.35773	-.18733
.87800	.00716	-.02881	.02804	49	.90240	-.16498		
	-.02119	.39884	-.20697			-.02059	.36920	-.14439
.92680	-.00089	.05916	-.01631	50	.95120	-.15909		
	-.02220	.39004	-.20113			-.07600	.37822	-.08309
.97560	-.00865	.14676	-.06261	51	1.00000	-.14183		
	-.02590	.28031	-.14014			-.07254	.38200	-.06929
1.02440	-.01557							
	-.02944							

VELOCITIES ON CENTER LINE

XV	VF	VW	XU	UF	UW
-.78165E+01	.48334E-02	-.41861E-02			
-.64734E+01	.58019E-02	-.46516E-02	-.71489E+01	-.10242E-02	-.39298E-03
-.54660E+01	.68195E-02	-.48291E-02	-.59719E+01	-.13779E-02	-.18801E-02
-.46825E+01	.78896E-02	-.50390E-02	-.50756E+01	-.18719E-02	-.38246E-02
-.40557E+01	.90129E-02	-.53548E-02	-.43700E+01	-.24890E-02	-.56849E-02
-.35428E+01	.10190E-01	-.57604E-02	-.37998E+01	-.32202E-02	-.73341E-02
-.31155E+01	.11421E-01	-.62175E-02	-.33296E+01	-.40606E-02	-.87452E-02
-.27538E+01	.12709E-01	-.66894E-02	-.29349E+01	-.50099E-02	-.99330E-02
-.24439E+01	.14058E-01	-.71493E-02	-.25991E+01	-.60725E-02	-.10932E-01
-.21753E+01	.15473E-01	-.75810E-02	-.23097E+01	-.72580E-02	-.11781E-01
-.19402E+01	.16960E-01	-.79768E-02	-.20578E+01	-.85807E-02	-.12513E-01
-.17328E+01	.18528E-01	-.83342E-02	-.18366E+01	-.10060E-01	-.13152E-01
-.15484E+01	.20184E-01	-.86544E-02	-.16407E+01	-.11722E-01	-.13718E-01
-.13835E+01	.21941E-01	-.89399E-02	-.14660E+01	-.13596E-01	-.14221E-01
-.12350E+01	.23811E-01	-.91941E-02	-.13093E+01	-.15723E-01	-.14671E-01
-.11007E+01	.25810E-01	-.94203E-02	-.11679E+01	-.18151E-01	-.15074E-01
-.97862E+00	.27955E-01	-.96217E-02	-.10397E+01	-.20939E-01	-.15435E-01
-.86713E+00	.30270E-01	-.98013E-02	-.92290E+00	-.24164E-01	-.15760E-01
-.76493E+00	.32784E-01	-.99615E-02	-.81606E+00	-.27923E-01	-.16052E-01
-.67091E+00	.35531E-01	-.10104E-01	-.71794E+00	-.32343E-01	-.16315E-01
-.58412E+00	.38560E-01	-.10232E-01	-.62753E+00	-.37594E-01	-.16552E-01
-.50376E+00	.41936E-01	-.10346E-01	-.54396E+00	-.43908E-01	-.16766E-01
-.42914E+00	.45749E-01	-.10447E-01	-.46647E+00	-.51611E-01	-.16959E-01
-.35967E+00	.50134E-01	-.10537E-01	-.39442E+00	-.61178E-01	-.17130E-01
-.29483E+00	.55298E-01	-.10618E-01	-.32726E+00	-.73342E-01	-.17280E-01
-.23417E+00	.61590E-01	-.10689E-01	-.26451E+00	-.89294E-01	-.17411E-01
-.17730E+00	.69645E-01	-.10751E-01	-.20574E+00	-.11117E+00	-.17523E-01
-.12388E+00	.80749E-01	-.10805E-01	-.15060E+00	-.14332E+00	-.17613E-01
-.73600E-01	.97794E-01	-.10852E-01	-.98745E-01	-.19631E+00	-.17672E-01
-.24800E-01	.12888E+00	-.10902E-01	-.49200E-01	-.29954E+00	-.17637E-01
.24000E-01	.65838E+00	-.11394E-01	-.40000E-03	-.42744E+00	-.17131E-01
	-.60217E+00	-.11245E-01		-.67458E+00	-.17131E-01
.72800E-01	.24158E+00	-.11105E-01	.48400E-01	.45648E+00	-.18290E-01
	-.20711E+00	-.11043E-01		.20793E-01	-.18290E-01
.12160E+00	.11919E+00	-.11303E-01	.97200E-01	.51950E+00	-.18435E-01
	-.14675E+00	-.11245E-01		.57883E-01	-.18435E-01
.17040E+00	.68804E-01	-.11350E-01	.14600E+00	.52721E+00	-.18358E-01
	-.10103E+00	-.11294E-01		.94778E-01	-.18358E-01
.21920E+00	.37442E-01	-.11371E-01	.19480E+00	.52212E+00	-.18334E-01
	-.65030E-01	-.11317E-01		.11538E+00	-.18334E-01
.26800E+00	.98117E-02	-.11402E-01	.24360E+00	.52502E+00	-.18372E-01
	-.36839E-01	-.11349E-01		.12244E+00	-.18372E-01
.31680E+00	-.10704E-01	-.11429E-01	.29240E+00	.52824E+00	-.18421E-01
	-.10904E-01	-.11376E-01		.12502E+00	-.18421E-01
.36560E+00	-.26083E-01	-.11448E-01	.34120E+00	.52914E+00	-.18481E-01
	.14715E-01	-.11395E-01		.12108E+00	-.18481E-01

.41440E+00	-.43824E-01	-.11476E-01	.39000E+00	.53553E+00	-.18562E-01
	.37057E-01	-.11422E-01		.10561E+00	-.18562E-01
.46320E+00	-.65517E-01	-.11522E-01	.43880E+00	.54950E+00	-.18645E-01
	.54735E-01	-.11467E-01		.82880E-01	-.18645E-01
.51200E+00	-.86136E-01	-.11579E-01	.48760E+00	.56392E+00	-.18715E-01
	.71495E-01	-.11522E-01		.59976E-01	-.18715E-01
.56080E+00	-.10817E+00	-.11653E-01	.53640E+00	.58023E+00	-.18778E-01
	.89358E-01	-.11595E-01		.34176E-01	-.18778E-01
.60960E+00	-.12456E+00	-.11745E-01	.58520E+00	.59062E+00	-.18817E-01
	.10365E+00	-.11685E-01		-.17804E-02	-.18817E-01
.65840E+00	.35439E-01	-.11838E-01	.63400E+00	.36253E+00	-.18861E-01
	.10876E+00	-.11776E-01		-.47076E-01	-.18861E-01
.70720E+00	-.10174E+00	-.12660E-01	.68280E+00	.21549E+00	-.19122E-01
	.10166E+00	-.12553E-01		-.95443E-01	-.19122E-01
.75600E+00	-.13789E+00	-.12706E-01	.73160E+00	.17282E+00	-.18294E-01
	.79899E-01	-.12596E-01		-.14046E+00	-.18294E-01
.80480E+00	-.15458E+00	-.12563E-01	.78040E+00	.12122E+00	-.17739E-01
	.51612E-01	-.12450E-01		-.17189E+00	-.17739E-01
.85360E+00	-.16466E+00	-.12405E-01	.82920E+00	.76041E-01	-.17442E-01
	.22666E-01	-.12291E-01		-.19113E+00	-.17442E-01
.90240E+00	-.16498E+00	-.12281E-01	.87800E+00	.28039E-01	-.17278E-01
	-.20592E-01	-.12166E-01		-.20697E+00	-.17278E-01
.95120E+00	-.15909E+00	-.12182E-01	.92680E+00	-.16313E-01	-.17186E-01
	-.76002E-01	-.12070E-01		-.20113E+00	-.17186E-01
.10000E+01	-.14163E+00	-.12076E-01	.97560E+00	-.62609E-01	-.17144E-01
	-.72540E-01	-.11968E-01		-.14014E+00	-.17144E-01
.10488E+01	-.77620E-01	-.11929E-01	.10244E+01	-.11135E+00	-.17100E-01
.10976E+01	-.66799E-01	-.11847E-01	.10732E+01	-.76554E-01	-.17002E-01
.11479E+01	-.59284E-01	-.11767E-01	.11227E+01	-.59943E-01	-.16911E-01
.12013E+01	-.53443E-01	-.11685E-01	.11746E+01	-.49094E-01	-.16812E-01
.12582E+01	-.48652E-01	-.11598E-01	.12297E+01	-.41081E-01	-.16701E-01
.13188E+01	-.44579E-01	-.11506E-01	.12885E+01	-.34798E-01	-.16574E-01
.13837E+01	-.41029E-01	-.11404E-01	.13512E+01	-.29707E-01	-.16427E-01
.14531E+01	-.37877E-01	-.11290E-01	.14184E+01	-.25494E-01	-.16258E-01
.15278E+01	-.35040E-01	-.11160E-01	.14904E+01	-.21957E-01	-.16062E-01
.16081E+01	-.32459E-01	-.11012E-01	.15679E+01	-.18956E-01	-.15836E-01
.16949E+01	-.30092E-01	-.10840E-01	.16515E+01	-.16391E-01	-.15574E-01
.17889E+01	-.27905E-01	-.10641E-01	.17419E+01	-.14185E-01	-.15273E-01
.18911E+01	-.25875E-01	-.10409E-01	.18400E+01	-.12280E-01	-.14925E-01
.20026E+01	-.23982E-01	-.10138E-01	.19468E+01	-.10630E-01	-.14526E-01
.21247E+01	-.22208E-01	-.98209E-02	.20636E+01	-.91969E-02	-.14066E-01
.22590E+01	-.20543E-01	-.94506E-02	.21918E+01	-.79513E-02	-.13536E-01
.24075E+01	-.18974E-01	-.90188E-02	.23332E+01	-.68686E-02	-.12924E-01
.25724E+01	-.17492E-01	-.85169E-02	.24899E+01	-.59292E-02	-.12218E-01
.27568E+01	-.16091E-01	-.79371E-02	.26645E+01	-.51172E-02	-.11399E-01
.29642E+01	-.14761E-01	-.72735E-02	.28604E+01	-.44211E-02	-.10444E-01
.31993E+01	-.13498E-01	-.65246E-02	.30816E+01	-.38337E-02	-.93235E-02
.34679E+01	-.12294E-01	-.56978E-02	.33334E+01	-.33531E-02	-.79950E-02
.37778E+01	-.11140E-01	-.48163E-02	.36227E+01	-.29854E-02	-.63987E-02
.41395E+01	-.10024E-01	-.39319E-02	.39584E+01	-.27497E-02	-.44478E-02

I	JMX	KMX	ISUP	NS	DPHIMX	DA
1	52	-1	0	111	-.38770E-02	0.
2	52	-1	0	111	.37163E-02	0.
3	52	-1	0	111	-.30487E-02	0.
4	52	-1	0	111	.26640E-02	0.
5	52	-1	0	111	-.21190E-02	0.
6	52	-1	0	111	.17805E-02	0.
7	52	-1	0	111	-.13820E-02	0.
8	53	-1	0	111	.11457E-02	0.
9	53	-1	0	111	-.90558E-03	0.
10	53	-1	0	111	.72971E-03	0.
11	54	-1	0	111	-.58210E-03	0.
12	54	-1	0	111	.46904E-03	0.
13	54	-1	0	111	-.37208E-03	0.
14	55	-1	0	111	.29874E-03	0.
15	55	-1	0	111	-.23880E-03	0.
16	55	-1	0	111	.19047E-03	0.
17	56	-1	0	111	-.15124E-03	0.
18	56	-1	0	111	.12347E-03	0.
19	56	-1	0	111	-.95437E-04	0.
20	56	-1	0	111	.79340E-04	0.
21	57	-1	0	111	-.60930E-04	0.
22	52	-1	0	111	.51205E-04	0.
23	58	-1	0	111	-.39412E-04	0.
24	44	1	1	111	.29864E-03	-.11581E-01
25	44	8	0	111	-.12614E-03	-.11581E-01
26	45	8	0	111	.62226E-04	-.11581E-01
27	46	10	0	111	.54555E-04	-.11581E-01
28	49	18	0	111	.31439E-04	-.11581E-01
29	44	1	1	111	.22222E-03	-.11414E-01
30	44	8	0	111	-.98535E-04	-.11414E-01
31	44	8	0	111	.66069E-04	-.11414E-01
32	45	10	0	111	.41065E-04	-.11414E-01
33	44	1	1	111	.12934E-03	-.11304E-01
34	46	1	0	112	.41907E-04	-.11304E-01
35	45	2	0	112	.10148E-03	-.11225E-01
36	45	1	0	112	.39001E-04	-.11225E-01
37	45	2	0	112	.65594E-04	-.11171E-01
38	45	1	0	112	.31122E-04	-.11171E-01
39	45	2	0	112	.39571E-04	-.11135E-01
40	44	1	1	112	.51630E-04	-.11108E-01
41	39	-1	0	112	-.26794E-04	-.11108E-01
42	44	8	0	112	.44215E-04	-.11094E-01
43	38	-1	0	112	-.23409E-04	-.11087E-01
44	37	-1	0	112	-.21082E-04	-.11084E-01
45	39	-1	0	112	-.18932E-04	-.11084E-01
46	38	-1	0	112	-.17072E-04	-.11087E-01
47	38	-1	0	112	-.15336E-04	-.11092E-01
48	36	-8	0	112	-.14035E-04	-.11098E-01
49	36	-9	0	112	-.13348E-04	-.11105E-01
50	36	-11	0	112	-.12752E-04	-.11111E-01
51	35	-12	0	112	-.12241E-04	-.11118E-01
52	34	-12	0	112	-.11781E-04	-.11125E-01
53	34	-13	0	112	-.11346E-04	-.11131E-01
54	33	-13	0	112	-.10932E-04	-.11137E-01
55	33	-14	0	112	-.10525E-04	-.11143E-01
56	32	-14	0	112	-.10150E-04	-.11148E-01
57	31	-14	0	112	-.97685E-05	-.11153E-01
58	30	-14	0	112	-.93831E-05	-.11158E-01
59	30	-15	0	112	-.90201E-05	-.11162E-01
60	29	-15	0	112	-.86597E-05	-.11166E-01
61	29	-15	0	112	-.83041E-05	-.11170E-01
62	29	-15	0	112	-.79499E-05	-.11174E-01
63	29	-15	0	112	-.76130E-05	-.11177E-01
64	28	-15	0	112	-.72905E-05	-.11180E-01
65	28	-15	0	112	-.69775E-05	-.11182E-01
66	28	-15	0	112	-.66714E-05	-.11185E-01
67	28	-16	0	112	-.63678E-05	-.11187E-01
68	28	-16	0	112	-.61147E-05	-.11190E-01
69	28	-16	0	112	-.58552E-05	-.11192E-01
70	28	-16	0	112	-.56121E-05	-.11193E-01
71	28	-16	0	112	-.53829E-05	-.11195E-01
72	28	-16	0	112	-.51642E-05	-.11197E-01
73	28	-16	0	112	-.49562E-05	-.11198E-01

EQUIVALENT FREE AIR (U AND V ARE PERTURBATIONS FROM UINF BUT NORMALIZED BY UREF)

ALPHA CORRECTION = -.11198E-01

X(J-.5)	YMOD	CP(INF)	U	J	X(J)	V	DELTA PHI	DELTA V
-.00040	0.00000	.80555	-.42654	31	.02400	.65814		
	0.00000	1.03680	-.67611			-.60215	.01218	1.26029
.04840	.03212	-.69260	.45795	32	.07280	.24168		
	-.02938	.11355	.01910			-.20691	.03360	.44859
.09720	.04391	-1.04716	.52049	33	.12160	.11908		
	-.03548	-.08143	.05608			-.14675	.05626	.26584
.14600	.04972	-1.09930	.52817	34	.17040	.06865		
	-.04664	-.17506	.09301			-.10108	.07749	.16973
.19480	.05307	-1.09849	.52310	35	.21920	.03727		
	-.05158	-.22806	.11362			-.06511	.09748	.10238
.24360	.05489	-1.10794	.52601	36	.26800	.00961		
	-.05475	-.24810	.12068			-.03695	.11726	.04656
.29240	.05536	-1.11535	.52924	37	.31680	-.01093		
	-.05656	-.25604	.12328			-.01104	.13707	.00011
.34120	.05483	-1.11664	.53015	38	.36560	-.02633		
	-.05710	-.24846	.11937			.01455	.15711	-.04089
.39000	.05354	-1.12818	.53657	39	.41440	-.04410		
	-.05639	-.21510	.10395			.03687	.17823	-.08097
.43880	.05139	-1.15347	.55058	40	.46320	-.06584		
	-.05459	-.16576	.08126			.05450	.20113	-.12034
.48760	.04818	-1.17793	.56506	41	.51200	-.08652		
	-.05193	-.11592	.05838			.07121	.22585	-.15772
.53640	.04395	-1.20445	.58145	42	.56080	-.10862		
	-.04845	-.05993	.03259			.08900	.25264	-.19762
.58520	.03865	-1.21854	.59195	43	.60960	-.12510		
	-.04411	.01629	-.00335			.10320	.28169	-.22831
.63400	.03255	-.77083	.36509	44	.65840	.03480		
	-.03907	.10879	-.04866			.10822	.30188	-.07342
.68280	.03425	-.46563	.22187	45	.70720	-.10323		
	-.03379	.20336	-.09728			.10034	.31746	-.20358
.73160	.02921	-.35231	.17696	46	.75600	-.13943		
	-.02889	.28487	-.14149			.07854	.33300	-.21797
.78040	.02240	-.23126	.12354	47	.80480	-.15598		
	-.02506	.33916	-.17239			.05040	.34744	-.20638
.82920	.01479	-.13099	.07745	48	.85360	-.16590		
	-.02260	.37162	-.19135			.02162	.36056	-.18752
.87800	.00670	-.03020	.02893	49	.90240	-.16610		
	-.02155	.39899	-.20705			-.02152	.37207	-.14458
.92680	-.00141	.05839	-.01576	50	.95120	-.16011		
	-.02260	.39011	-.20113			-.07683	.38112	-.08328
.97560	-.00922	.14645	-.06231	51	1.00000	-.14275		
	-.02635	.28027	-.14007			-.07327	.38491	-.06948
1.02440	-.01619							
	-.02992							

EXPERIMENTAL CP BASED ON CORRECTED AMINF, CL = .78462

X	CP(INF)
.04840	-.71661
	.12171
.09720	-1.05269
	-.08301
.14600	-1.09972
	-.17723
.19480	-1.09930
	-.23090
.24360	-1.10762
	-.25149
.29240	-1.11404
	-.25993
.34120	-1.11456
	-.25281
.39000	-1.12525
	-.21979
.43880	-1.14989
	-.17071
.48760	-1.17380
	-.12111
.53640	-1.19993
	-.06537
.58520	-1.21982
	.01067
.63400	-.76277
	.10321
.68280	-.44659
	.19811
.73160	-.34192
	.28018
.78040	-.22580
	.33509
.82920	-.12814
	.36811
.87800	-.02888
	.39607
.92680	.05872
	.38791
.97560	.14599
	.27849

REFERENCES

1. Kemp, William B., Jr.: Toward the Correctable-Interference Transonic Wind Tunnel. AIAA 9th Aerodynamic Testing Conference, 1976, pp. 31-38.

2. Kemp, William B., Jr.: Transonic Assessment of Two-Dimensional Wind Tunnel Wall Interference Using Measured Wall Pressures. NASA Conference Publication 2045, March 1978, pp. 473-486.

3. Klunker, E. B.: Contribution to Methods for Calculating the Flow About Thin Lifting Wings at Transonic Speeds - Analytic Expressions for the Far Field. NASA TN D-6530, 1971.

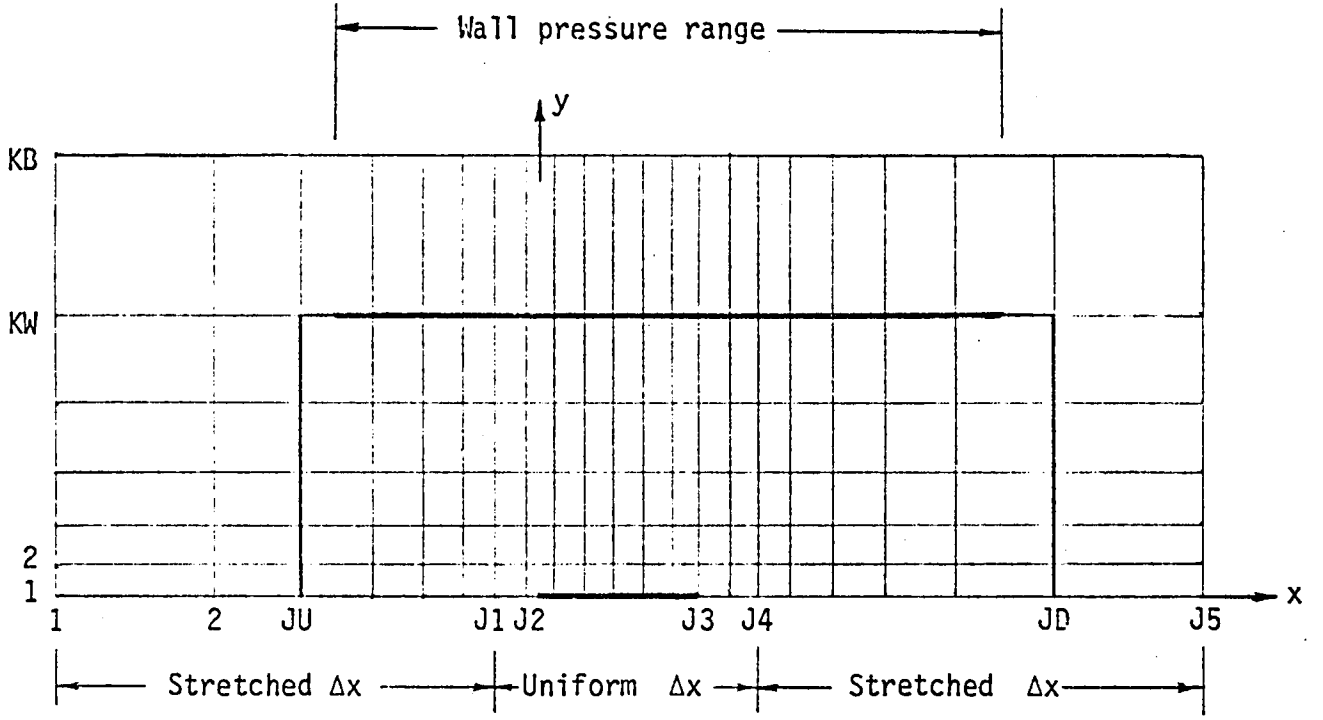

Figure 1.- Schematic representation of upper half of computational grid. Lower half is mirror image about x axis.

1. Report No.	2. Government Accession No.	3. Recipient's Catalog No.
NASA TM-81819		

4. Title and Subtitle	5. Report Date
TWINTAN: A Program for Transonic Wall Interference Assessment in Two-Dimensional Wind Tunnels	May 1980
	6. Performing Organization Code
7. Author(s)	8. Performing Organization Report No.
William B. Kemp, Jr.	
9. Performing Organization Name and Address	10. Work Unit No.
NASA Langley Research Center Hampton, Virginia 23665	505-31-53-03
	11. Contract or Grant No.
	13. Type of Report and Period Covered
12. Sponsoring Agency Name and Address	Technical Memorandum
National Aeronautics and Space Administration Washington, DC 20546	14. Sponsoring Agency Code

15. Supplementary Notes

16. Abstract

A method for assessing the wall interference in transonic two-dimensional wind-tunnel tests has been developed and implemented in a computer program. The method involves three successive solutions of the transonic small disturbance potential equation to define the wind-tunnel flow, the perturbation attributable to the model, and the equivalent free air flow around the model. Required input includes pressure distributions on the model and along the top and bottom tunnel walls which are used as boundary conditions for the wind-tunnel flow. The wall-induced perturbation field is determined as the difference between the perturbation in the tunnel flow solution and the perturbation attributable to the model. The methodology used in the program is described and detailed descriptions of the computer program input and output are presented. Input and output for a sample case are given in an appendix.

17. Key Words (Suggested by Author(s))

Wall interference
Boundary effects
Boundary corrections
Wind tunnels
Transonic flow

18. Distribution Statement

Unclassified - Unlimited

Subject category 09

19. Security Classif. (of this report)	20. Security Classif. (of this page)	21. No. of Pages	22. Price*
Unclassified	Unclassified	38	$4.50

For sale by the National Technical Information Service, Springfield, Virginia 22161